IRSTI 29.27.49 https://doi.org/10.26577/10.26577/RCPh.2021.v77.i2.04

A.B. Tazhen[1]*, M.K. Dosbolayev[2]

[1]Al-Farabi Kazakh National University, Kazakhstan, Almaty
[2]Scientific Research Institute of Experimental and Theoretical Physics, Kazakhstan, Almaty
*e-mail: aigerim_kz271295@mail.ru

MEASURING THE SELF-GENERATED MAGNETIC FIELD AND THE VELOCITY OF PLASMA FLOW IN A PULSED PLASMA ACCELERATOR

In phase of radial compression the unsteady plasma flow at the exit of a pulsed plasma accelerators is related to the generation of fast high-energy charged particle beams, to plasma density perturbations, to the internal plasma pressure is opposite to the external magnetic pressure ($B^2/2\mu_0$) associated with plasma column's self-generated magnetic field. The last one listed above is of particular interest. The investigation of the magnetic field of plasma flow relatively gives information about the above mutually close factors cause to plasma flow instability.

In this paper a miniature high-frequency magnetic probe are made for measuring and further investigating the pulsed self-generated magnetic field of plasma flow, in particular, at the exit of the accelerator in an experimental setup of PPA (located in KazNU, IETP). The magnetic probe dimensions are following: coil diameter is 2,12 *mm*, number of turns is 7, copper wire diameter is 150 μm, and winding length is 1, 1 *mm*. The coil inductance is about 0,113 μH and the temporal resolution of the magnetic probe is 2,3 *ns*. The magnetic probe was calibrated using a Hall sensor on the magnetic field of a multi-layered solenoid connected to an alternating power source of 15 A. Thus, the evaluated measurement error of the probe was no more than 10%.

Key words: pulsed plasma accelerator, plasma flow, self-generated magnetic field of plasma flow, magnetic probe.

Ә.Б. Тәжен[1]*, М.Қ. Досболаев[2]

[1]Әл-Фараби атындағы Қазақ ұлттық университеті, Қазақстан, Алматы қ.
[2]Эксперименттік және теориялық физика ғылыми-зерттеу институты, Қазақстан, Алматы қ.
*e-mail: aigerim_kz271295@mail.ru

Импульстік плазмалық үдеткіштегі плазмалық ағынның өздік магниттік өрісін және жылдамдығын өлшеу

Радиалды сығылу кезеңіндегі плазмалық үдеткіштердің шығысындағы плазмалық ағынның тұрақсыздығы көптеген факторларға байланысты. Олар, өте жылдам, жоғары энергиялы зарядталған бөлшектердің, плазмалық белдіктің өздік магниттік өрісі тудыратын магниттік қысымға қарсы плазманың ішкі қысымының пайда болуы және плазма тығыздығының біртекті таралмауы. Солардың ішінде плазмалық ағынның өздік магниттік өрісін зерттеу ерекше қызығушылық тудырады, себебі ол жоғарыда аталған өзара байланысқан факторлар туралы салыстырмалы түрде ақпарат бере алады.

Бұл жұмыста ИПУ (ҚазҰУ, ЭТФҒЗИ) эксперименттік қондырғыда, атап айтқанда плазмалық үдеткіштің шығысындағы плазмалық ағынның өздік магниттік өрісін өлшеу үшін және зерттеу үшін, жоғары жиілікті, шағын магниттік зонд жасалды. Магниттік зондтың геометриялық өлшемдері келесідей: катушканың диаметрі 2,12 мм, орам саны 7, мыс сымның диаметрі 150 мкм, орамның ұзындығы 1,1 мм. Өлшеуіш катушканың индуктивтілігі 0,113 мкГн, зондтың сезгіштігі 2,3 нс құрайды. Сонымен қатар магниттік зонд шамасы 15 А тең айнымалы ток көзіне қосылған көп қабатты соленоидтың Холл сенсорымен анықталған магниттік өрісінде калибрленді. Калибрлеу нәтижесі көрсеткендей, зондтың өлшеу қателігі 10% аспады.

Түйін сөздер: импульстік плазмалық үдеткіш, плазмалық ағын, плазмалық ағынның өздік магнит өрісі, магниттік зонд.

 © 2021 Al-Farabi Kazakh National University

А.Б. Тажен*, М.К. Досболаев

[1]Казахский **н**ациональный **у**ниверситет имени аль-Фараби, Казахстан, **г.** Алматы
[2]Научно-исследовательский институт экспериментальной и теоретической физики, Казахстан, **г.** Алматы
*e-mail: aigerim_kz271295@mail.ru

Измерение собственного магнитного поля и скорости плазменного потока в импульсном плазменном ускорителе

Нестабильное течение плазменного сгустка на выходе из плазменных ускорителей в стадии радиального сжатия связано со многими факторами: генерацией высокоэнергичных пучков заряженных частиц, возмущением плотности, внутренним давлением плазмы обратного по направлению внешнему давление собственного магнитного поля плазменного шнура. Особый интерес из них вызывает последнее, исследование собственного магнитного поля плазменного потока, который относительно дает информацию и о вышесказанных взаимосвязанных между собой факторах.

В этой работе нами был изготовлен высокочастотный магнитный зонд малого размера для измерения и дальнейшего исследования импульсного магнитного поля плазменного потока в экспериментальной установке ИПУ (КазНУ, НИИЭТФ), в частности на выходе из ускорителя. Магнитный зонд имеет следующие геометрические размеры: диаметр катушки – 2,12 мм, число витков – 7, диаметр медного провода – 150 мкм, длина намотки – 1,1 мм. Индуктивность катушки составляет 0,113 мкГн, время отклика магнитного зонда равна 2,3 нс. Магнитный зонд был откалиброван с помощью датчика Холла на магнитном поле многослойного соленоида, подключенного к переменному току силой 15 А. Таким образом, погрешность измерения составляет не более 10%.

Ключевые слова: импульсный плазменный ускоритель, плазменный поток, собственное магнитное поле плазменного потока, магнитный зонд.

Introduction

Coaxial plasma accelerators having energy more than 5 *J* and 1 *MJ* are widely used in a various types of applications for scientific and applied assignments. For instance, they are used in astrophysics, thermonuclear power engineering, nanotechnology, plasma chemistry, radiography and other fields [1-5].

The operation principle of plasma accelerators is based on the following: a vacuum chamber of accelerators is filled with a working gas at low pressure, usually, it is a D-T gas mixture to generate high-energy neutrons and X-rays [6-8]. During discharging the capacitors connecting to the coaxial electrodes, the current flowing between anode and cathode ionizes gas. Then an ionized gas develops to plasma column and this process can be divided into three stages: 1) gas breakdown and formation of plasma sheath, 2) axial acceleration of plasma shetah, and 3) radial compression of plasma sheath [9]. Detailed description gives below.

When the gas breakdown takes place, thin spark channels are formed between anode and cathode. These channels merge to each other and form a homogeneous plasma sheath [10, 11]. The current density in the plasma sheath is sufficiently high, that can create a strong magnetic field. Due to this, an electrodynamic force $\mathbf{J} \times \mathbf{B}$ appears, corresponding to Ampere's law. This electrodynamic force has an axial component; consequently, the plasma sheath is accelerated along the axis of the vacuum chamber towards the open end of a pulsed plasma accelerator. Then plasma flow is strongly compressed radially at the exit of the accelerator by its self-generated magnetic field.

In the stages of axial acceleration and radial compression, plasma column becomes more inhomogeneous and unstable due to particles density perturbations in plasma flow related to plasma oscillations and internal plasma pressure is opposite to the magnetic pressure [12]. Plasma instabilities are well investigated theoretically and numerically by MHD model [13, 14], however, there are a few experimental studies. An experimental investigations of plasma flow in a pulsed plasma accelerators and the plasma acceleration dynamics are possible, for this it is necessary to obtain a map of the current density, magnetic field distributions and other especially important plasma parameters (charged particles density, plasma flow energy and energy density, etc.) or to study the accelerated plasma sheath dynamics (speed, acceleration, etc.).

There are various types of methods for plasma flow diagnostics in a pulsed plasma accelerators: laser diagnostics, spectral diagnostics, electric probes, magnetic probes and etc.

Using magnetic probes, it is possible to measure the magnitude of self-generated magnetic field and velocity of plasma flow. Magnetic probes are miniature measuring coils. The operation principle of magnetic probes based on Faraday's law of electromagnetic induction [15-17]. According Faraday's law, the magnetic field, which is measured causes to EMF in the coils of a magnetic probe, which has an area S and a number of turns n. As can be seen from expression (1), the EMF with a magnitude of magnetic field related as follows:

$$\varepsilon = nS\frac{dB}{dt}. \quad (1)$$

Since the EMF is proportional to the derivative of magnetic field, it must be integrated. For this, an integrating electrical circuit (RC) is connected between a probe and an oscilloscope. The capacitance and resistivity of the capacitor and resistor are chosen so that the integration constant $\tau = RC$ is longer than the time of the ongoing process, but so as not to reduce the amplitude value of an input signal. In this case, the expression for an output signal (2) is written as follows:

$$\varepsilon = nS\frac{B}{RC}. \quad (2)$$

A magnetic probe has some privileges; they are short temporal resolution time of the order of several nano and microseconds, sensitivity to high-frequency oscillations, which makes it possible to use them in plasma installations operating in a pulsed mode.

The temporal resolution time of magnetic probes is obtained by the expression (3) [18]:

$$\tau = \frac{L}{R_0}, \quad (3)$$

where L is the coil inductance, it depends on the radius (r) and the number of turns of the coil (n), R_0 is the impedance of a coaxial cable. As can be seen from (3), the temporal resolution time of measurements with a magnetic probe not only depends on the choice of the parameter τ, but also on the coil inductance. When the amount of number of turns is high and the radius of the coil is large, the inductance of magnetic probes increases, due to which the temporal resolution time of the probe becomes high. Therefore, to manufacture the magnetic probe and to use it in measurements, it is necessary to take into account all the above disadvantages.

Experimental setup

The experimental setup is a coaxial pulsed plasma accelerator with a stored energy on capacitors of about 25 *kJ*. The vacuum chamber of the accelerator is made of stainless steel, inside the vacuum chamber there is a coaxial system of electrodes. Furthermore, except vacuum chamber and the system of electrodes, the experimental setup includes the following units: a pumping system including fore vacuum and diffusion vacuum pumps, a high-voltage power supply, a battery of storage capacitors, and a vacuum discharger [19-25]. A principle scheme of the experimental setup is shown in Fig. 1.

The total capacity of the capacitor bank is 1440 μF, the operating voltage is in the range of 2-6 *kV*, and the operating pressure is in the range of 10 *mTorr* – 1 *Torr*. Moreover, other types of gases can be injected into the vacuum chamber: argon, hydrogen, etc. For this, there is a special system for gas inlet. In this paper, experiments were performed with a residual air at low pressure.

Magnetic probe design

The inductive coil of the magnetic probe has 7 turns (copper wire is used), which were turned on a glass tube with an outer diameter of 2,12 *mm*. The measuring coil is placed inside a dielectric tube for electrostatic screening to reduce the influence of electric fields created by charged plasma particles, electrons and ions. The magnetic probe is connected to the LeCroy 354A oscilloscope (500 *MHz* bandwidth) through a coaxial cable with a characteristic impedance of 50 *Ohms*, between them there is an integrator. The integration time equal to 5,4 μs. The ends of the measuring coil are covered with a dielectric film to avoid electrical noises.

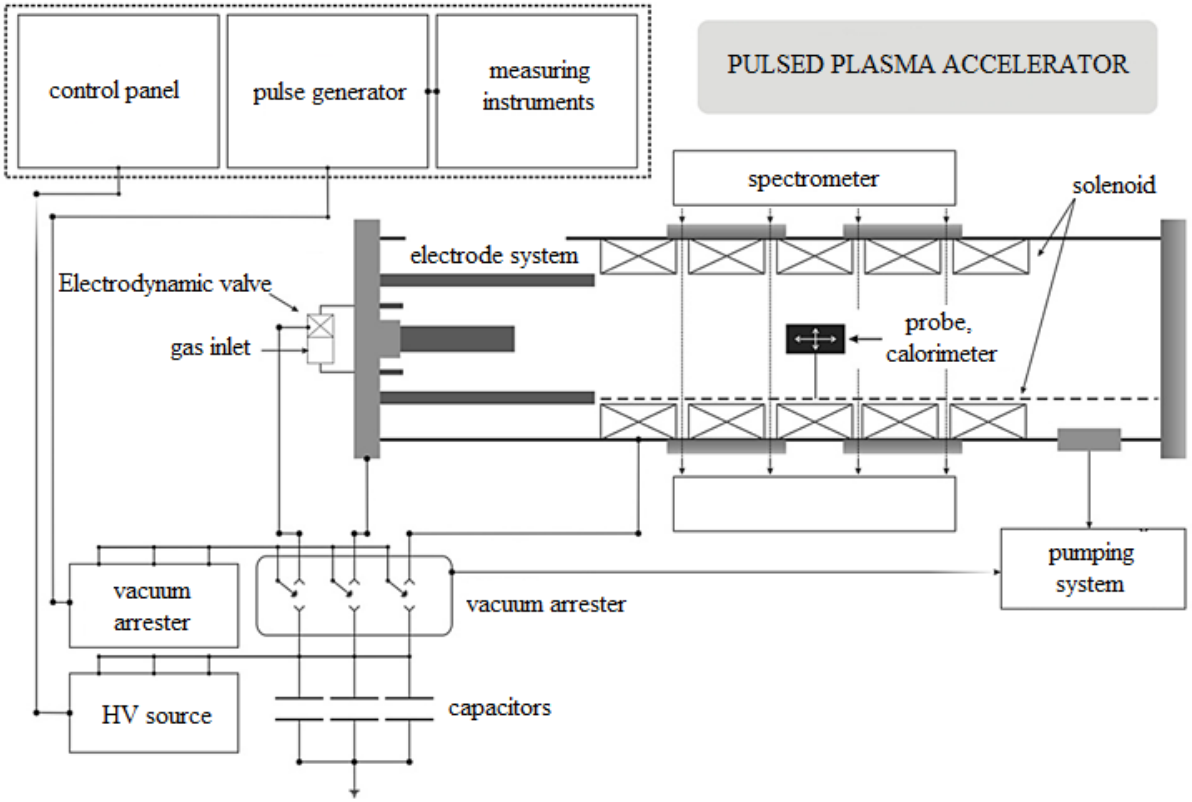

Figure 1 – Principle scheme of an experimental setup of a pulsed plasma accelerator

Magnetic probe calibration

The magnetic probe was calibrated using a multi-layered solenoid. The solenoid was connected to an alternating current source. The current in the solenoid was measured with a clamp meter, which was I ~ 5-15 A. An alternating uniform magnetic field is created in the center of the solenoid, where the measurement takes place. The relation between the amplitude value of the EMF at the ends of the probe and the magnetic field of a multi-layered solenoid is expressed as follows (1):

$$\varepsilon_0 = nS\omega B_0 = kB_0 \qquad (4)$$

where $\omega = 2\pi\nu$ is the cyclic frequency of the alternating current. To measure B_0, a 49E852X Hall sensor is used for ± 1000 *G*. The Hall sensor and magnetic probe both were connected directly to the oscilloscope. The oscillograms of the voltage across the sensor and the magnetic probe obtained experimentally are shown in Fig. 2.

In the technical support of the Hall sensor, a calibration curve is presented, which we used to obtain value of B_0. As a result, the measured value of the magnetic field in the center of the multi-layered solenoid by the Hall sensor at I ~ 5A was about 0,1 T. The value of the same field measured with a magnetic probe according to expression (4) was 0,09 *T*. It follows from this that the measurement error of the magnetic probe is: Δ = 0,01, about 1%. If we take into account the measurement errors of the Hall sensor from the technical support and other devices (including the experimentator), then the measurement error does not exceed 10%.

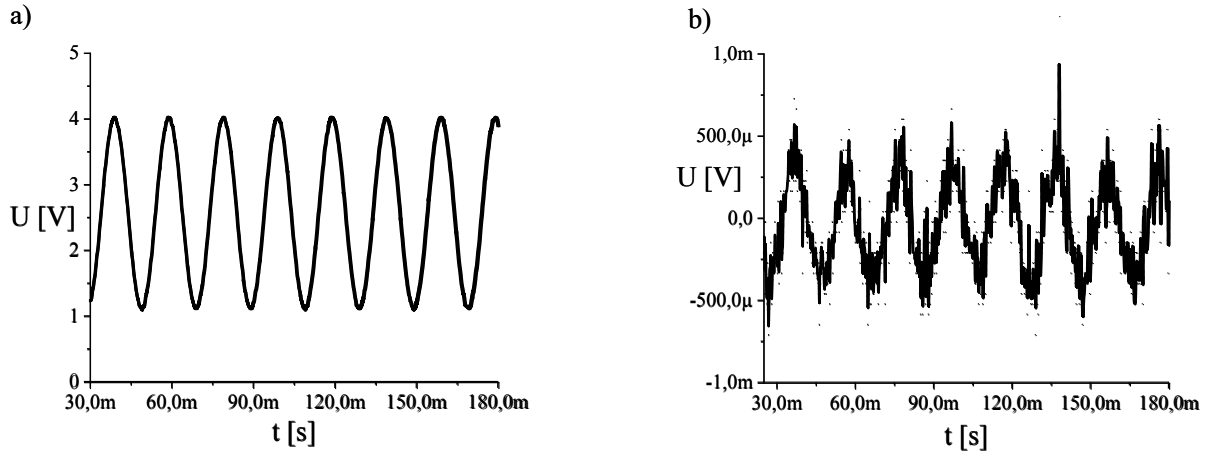

Figure 2 – Output signal that comes out from a) a Hall sensor and b) a magnetic probe

Results and discussions

Measuring the self-generated magnetic field magnitude of plasma flow in the PPA. A magnetic probe is placed near the pulsed plasma accelerator coaxial system of electrodes at a distance of 6 *cm*. An axis of the measuring coil of a magnetic probe is adjusted vertically to an axis of the cylindrical vacuum chamber, see Fig. 3. Before conducting the experiments, plasma accelerator vacuum chamber was pre-pumped to a pressure of about 10 *mTorr*. The measurements were carried out under the following conditions: a) at a constant charging voltage of capacitors $U = 3$ *kV* and at various gas pressures, in our case the residual air pressures are 30-260 *mTorr*; b) at a constant gas pressure $p = 40$ *mTorr* and at different charging voltages of capacitors 2-5 *kV*. In Fig. 3, the typical oscillograms of a current waveform of the PPA (solid curve) obtained using a Rogowski coil, a self-generated magnetic field derivative *dB*/*dt* curve (dashed line) and a curve of magnetic field magnitude (dot-dotted curve), respectively, obtained using a magnetic probe with and with absence the integrator (integration time constant is $\tau = 5{,}4$ *µs*) are presented.

The current waveform of the PPA (see Fig. 3) is a damped sinusoidal signal. At the moment when current would rise, the energy stored on the storage capacitors is transmitted to the coaxial electrodes thereby the residual air filling the interelectrode space is ionized and a plasma sheath is formed. The plasma lifetime was obtained from the current waveform curve, which was of ~ 300 *µs*. Since a magnetic probe is placed at 6 *cm* distance from the coaxial electrodes, between two output voltage signals obtained from a Rogowski coil and a magnetic probe, a time shift takes place, as can be seen in Fig. 3 that corresponds the axial acceleration of plasma sheath.

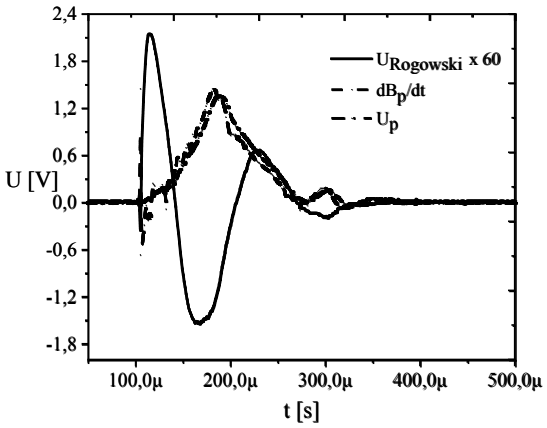

Figure 3 – Typical oscillograms obtained at pressure $p = 40$ *mTorr* and charging voltage $U = 5$ *kV* from a Rogowski coil, magnetic probe with and with absence integrator

By processing the current waveforms of the PPA, which is obtained at different values of the charging voltages, the current voltage curve of an experimental setup was plotted, see Fig. 4.

As seen from Fig. 4, when the charging voltage of storage capacitors increase the discharge current in the PPA circuit increases linearly, since the plasma has good conductivity, its resistance causes insignificant affect on the total resistance of the PPA circuit, respectively, on the current flowing through this circuit. Moreover rising of current is related with an increase of electrical field in space

between the coaxial electrodes; consequently, due to this a large number of ionization acts of gas take place. The positive ions and electrons appeared after ionization provides the rising of plasma conductivity.

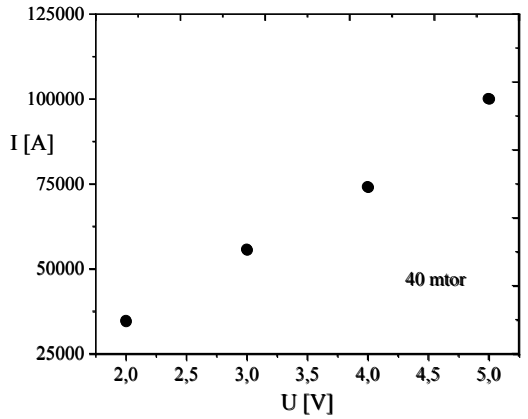

Figure 4 – Current voltage curve of an experimental setup

Using the oscillograms of output signals from a magnetic probe the following what were measured was self-generated magnetic field values of plasma flow at the exit of the coaxial system of electrodes (at a distance $L = 6$ *cm*). Measurements were carried out depending on the gas pressure and charging voltages of capacitors. Results are shown in Fig. 5 and Fig. 6.

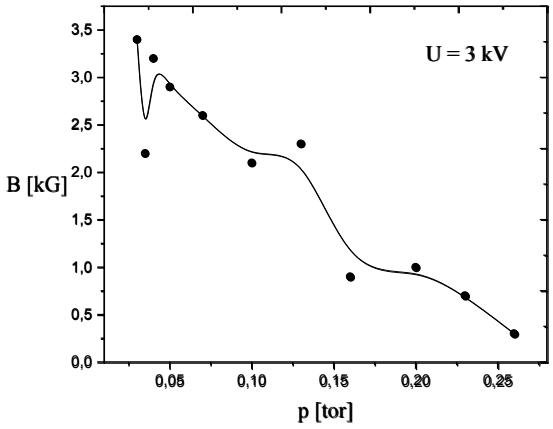

Figure 5 – Dependence of self-generated magnetic field values of plasma flow on the gas pressures

As shown in Fig. 5, dependence self-generated magnetic field value of plasma flow on a gas pressure is nonlinear; notwithstanding, it can be seen from the curve that the value of magnetic field decrease when increase the working gas pressure. Plasma parameters, including its magnetic field depend on energy putting into the discharge. Energy putting into the discharge sufficient to ionize a gas defines as a function of gas pressure according to Paschen's law, when the voltage and distance between two electrodes not changed. Moreover energy putting into the discharge can be depended on other factors, for example, the charged particles loss as plasma sheath expands and approaches the outer electrode in gas breakdown stage, dissipation of plasma energy and etc.

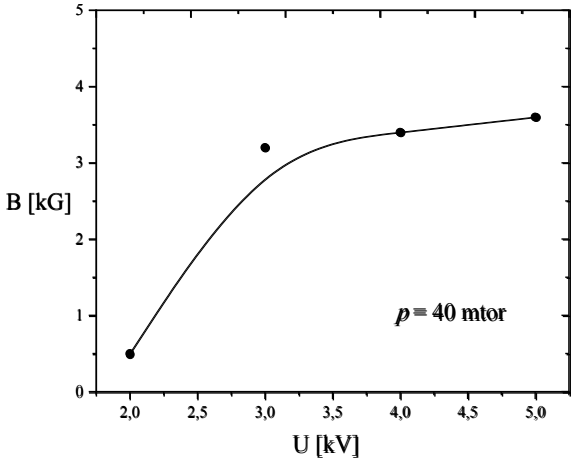

Figure 6 – Dependence of self-generated magnetic field values of plasma flow on the charging voltages of capacitors

It seen from Fig. 6 that when charging voltages of storage capacitors increase, the value of the of self-generated magnetic field of plasma flow also increases, since magnetic field of plasma flow depends on the plasma current density, therefore, when the charging voltage is high, then the strong electrical field appeared between electrodes provide to intensive ionization gas and formation a large number of charges. These charges are the primary carriers of the discharge current in plasma column. However, as seen from Fig. 6 at extremely low charging voltage of storage capacitors ~ 2 *kV*, the values of self-generated magnetic field of plasma flow substantially decrease in our experiments. Analyzing this result, it was revealed that the transfer of energy from the capacitors to the electrodes was related with on the operation and conductivity of a vacuum arrester. This of course declines the operation characteristics of an accelerator since transmitted to the electrode the part of the energy is lost for the ignition of the vacuum arrester.

Moreover in this work the processes of the plasma flow breakdown to separate discharges were observed. In the experiment the plasma flow breakdown took place especially at high pressures and low charging voltages, see Fig. 7.

Measuring the plasma flow velocity in the PPA. To measure the plasma flow velocity two same magnetic probes were used. The distance between the probes was 17,5 cm. The measurements were also carried out under two different conditions, as in the previous experiment. One of the examples of oscillograms obtained from two probes is shown in Fig. 8.

Since the magnetic probes are at a certain distance, then on each of the magnetic probes EMF occurs at different times. EMF first appears on the probe, which is closer to the system of coaxial electrodes, $p1$, and then on the probe $p2$, as seen in Fig. 8. Plasma flow velocities were calculated by measuring the time difference, depending on the gas pressure and the charging voltage of storage capacitors. The results are shown in Fig. 9 and Fig. 10.

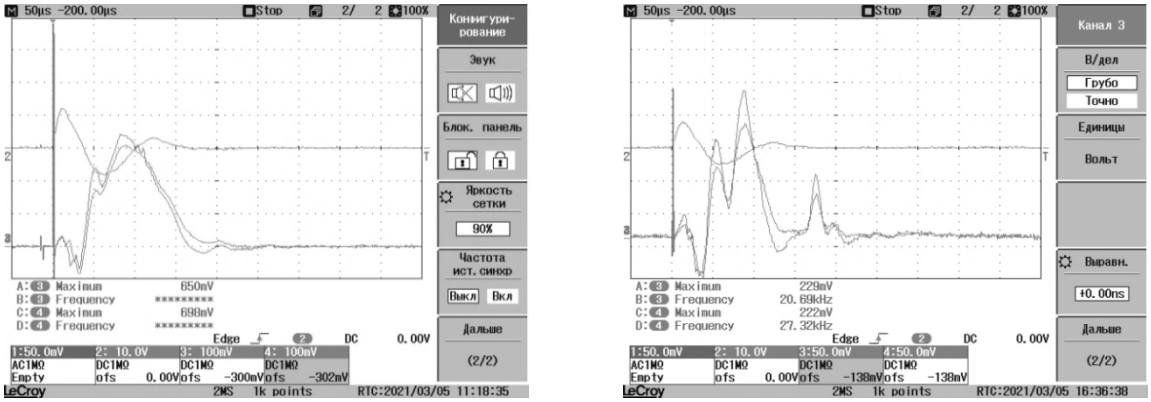

a) b)

a) 3 *kV*, 40 *mTorr*, b) 2 *kV*, 40 *mTorr*

Figure 7 – Pictures of plasma flow breakdown

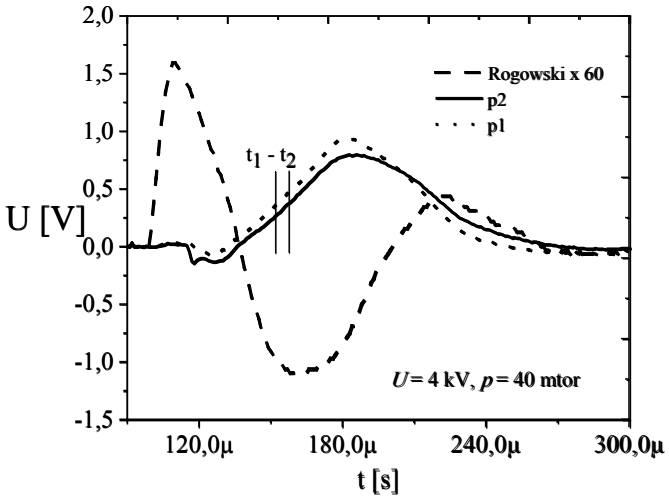

Figure 8 – Output voltage curves of two magnetic probes

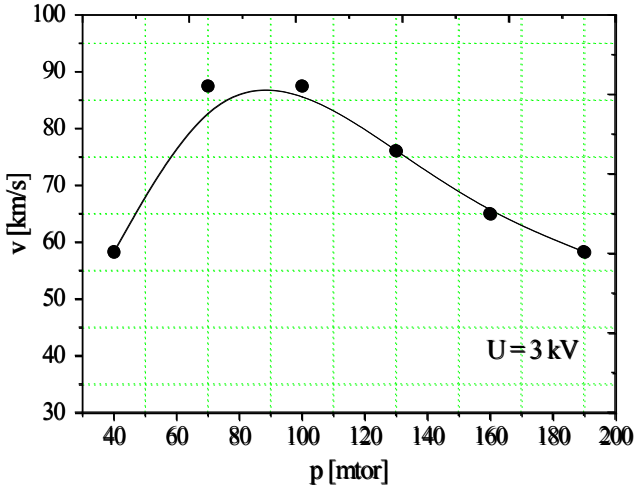

Figure 9 – Dependence of the plasma flow velocity on the gas pressures

According to accelerating force **J** × **B**, the high plasma current density provides the increasing of plasma flow velocity. Current density depends nonlinearly on the gas pressure corresponding to Paschen's law, as mentioned above; therefore the dependence of the plasma flow velocity on the gas pressures is also nonlinear. As seen in Fig. 9 there is a point of gas pressure with the maximum value of plasma flow velocity and at this point the pressure will be optimal for a pulsed plasma accelerator with charging voltage of capacitors is 3 *kV*.

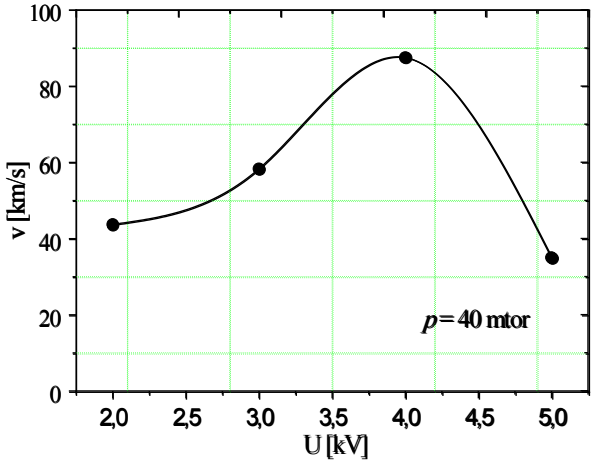

Figure 10 – Dependence of the plasma flow velocity on the charging voltages of capacitors

As seen from Fig. 10, with an increase in the voltage across the storage capacitors, the plasma flow velocity increases, however at high voltages, the velocity decreases instantly. It was an uncontemplated experimental result. According to this we assumed that perhaps it is related with an increase in the mass of plasma sheath, forasmuch as at high charging voltage of capacitors the sufficiently large number of ionization acts takes place and the density of positive ions increases. The mass of ions heavier than electron mass; therefore, the mass of plasma flow is majority concentrated on positive ions.

Conclusion

In this work, the self-generated magnetic field magnitude and the velocity of plasma flow in a pulsed plasma accelerator were investigated using a magnetic probe. The calibration of a magnetic

probe was carried out in an alternating magnetic field of ~ 0,1 T, what was measured by the Hall 49E852X sensor. According to the calibration results, the measurement error of a magnetic probe taking into account the Hall sensor's error was about 10%.

In a vacuum chamber of the PPA magnetic probes were placed at a distance of 6 cm and 23,5 cm of the end of coaxial electrodes, consequently, the distance between two probes was 17,5 cm. At first, depending on the gas pressures and charging voltages of storage capacitors, the values of the self-generated magnetic field of plasma flow were measured. It was found that the values of the self-generated magnetic field of plasma flow gradually decreases with an increase in the gas pressure and increases with an increase the charging voltage of capacitors. In the second case, using two identical magnetic probes, the plasma flow velocities were measured and its dependence on the gas pressures and the charging voltages of capacitors was obtained. The obtained graphs had complicated characteristic. From these graphs, it follows that with an increasing the charging voltage, the plasma flow velocity increases, however at a large value of charging voltage, in our experiments of 5 kV the velocity decreased. We assume that it perhaps depends on mass of plasma flow. Moreover in the case when the charging voltage of capacitors and the distance between two electrodes are not changed, according to Paschen's law, the plasma flow velocity at a certain gas pressure have a maximum value.

Funding

This work was supported by the Ministry of Education and Science of the Republic of Kazakhstan (project no. IRN AP09259081).

References

1 Yousefi H.R., Thornhill W., Sakai J.I., Nishino Y., Ito H., Masugata K. Dense plasma focus for laboratory astrophysics //Iranian Phys. Journal. – 2009. – Vol.2. – P.17-20.

2 Lerner E.J., Murali S.K., Blake A.M., Shannon D.M., Roesse F.J.V. Fusion reaction scaling in a mega-amp dense plasma focus //Nukleonika. – 2012. – Vol.57. – P.205-209.

3 Dosbolayev M.K., Utegenov A.U., Tazhen A.B., Ramazanov T.S. Investigation of dust formation in fusion reactors by pulsed plasma accelerator //Laser and Particle Beams. –2017. – Vol.35. – P.741-749.

4 Zdunek K., Nowakowska-Langier K., Chodun R., Okrasa S., Rabinski M., Dora J., Domanowski P., Halarowicz J. Impulse Plasma In Surface Engineering – a review //Journal of Phys.: Conference Series. – 2014. – Vol.564. – P.012007.

5 Gribkov V.A., Borovitskaya I.V., Demina E.V., Kazilin E.E., Latyshev S.V., Maslyaev S.A., Pimenov V.N., Laas T., Paduch M., Rogozhkin S.V. Application of dense plasma focus devices and lasers in the radiation material sciences for the goals of inertial fusion beyond ignition // Matter and Radiation at Extremes. – 2020. – Vol.5. – P.045403.

6 Chung S.R., Behbahani R.A., Xiao C. Charged particles and x-ray emission studies on a dense plasma focus device // Incorporating Plasma Sci. and Plasma Techn. – 2020. – Vol.175, P.1015-1020.

7 Jain J., Moreno J., Davis S., Bora B., Pavez C., Avaria G., Soto L. Experimental measurements of high-energy photons in X-rays pulses emitted from a hundred joules plasma focus device and its interpretations // Results in Phys. – 2020. – Vol.16. – P.102915.

8 Castillo-Mejía F., Gamboa-de Buen I., Herrera-Velázquezand J.J.E., Rangel-Gutiérrez J. Neutron emission characterisation at the FN-II Dense Plasma Focus // Journal of Phys.: Conference Series. – 2014. – Vol.511. – P.012021.

9 Scholz M., Bienkowska B., Ivanova-Stanik I., Karpinski L., Miklaszewski R., Paduch M., Stepniewski W., Tomaszewski K. The physics of a plasma focus // Czechoslovak Journal of Phys. – 2004. – Vol.54. – P.C170-185.

10 Kubes P., Paduch M., Cikhardt J., Cikhardtova B., Klir D., Kravarik J., Rezac K., Zielinska E., Sadowski M.J., Szymaszek A., Tomaszewski K., Zaloga D. Filamentation in the pinched column of the dense plasma focus // Phys. of Plasmas. – 2017. – Vol.24. – P.032706.

11 Kubes P., Paduch M., Cikhardt J., Klir D., Kravarik J., Rezac K., Cikhardtova B., Kortanek J. and Zielinska E. The influence of the nitrogen admixture on the evolution of a deuterium pinch column // Plasma Phys. and Controlled Fusion. – 2016. – Vol.58. – P.045005.

12 Liu J.X., Sears J., McMahon M., Tummel K., Cooper C., Higginson D., Shaw B., Povilus A., Link A., Schmidt A. Seeding the m = 0 instability in dense plasma focus Z-pinches with a hollow anode // Plasma Phys. – 2016. – P.1-8.

13 Narkis J., Hahn E.N., Lowe D.R., Housley D., Conti F., Beg F.N. Magnetohydrodynamic simulations of a megaampere-class Kr-doped deuterium dense plasma focus // Physics of Plasmas. – 2021. – Vol.28. – P.022707.

14 Beresnyak A., Giuliani J., Richardson S., Jackson S., Swanekamp S., Schumer J., Commisso R., Mosher D., Weber B. Simulations of a Dense Plasma Focus on a High-Impedance Generator // IEEE Transactions on Plasma Science. – 2018. – Vol.46. – P.3881 – 3885.

15 Saw S.H., Akel M., Lee P.C.K., Ong S.T., Mohamad S.N., Ismail F.D., Nawi N.D., Devi K., Sabri R.M., Baijan A.H., Ali J., Lee S. Magnetic Probe Measurements in INTI Plasma Focus to Determine Dependence of Axial Speed with Pressure in Neon // Journal of Fusion Energy. – 2012. – Vol.31. – P.1-6.

16 Piriaei D., Javadi S., Mahabadi T.D., Yousefi H.R., Salar Elahi A. and Ghoranneviss M. The influence of the cathode array and the pressure variations on the current sheath dynamics of a small plasma focus device in the presence of an axial magnetic probe // Physics of Plasmas. – 2017. – Vol.24. – P.043504.

17 El-Sayeda H.A., Allama T.M., Soliman H.M. Plasma Current Sheath Shape and Trapping Efficiency in the 2.2-kJ EAEA-PF1 Plasma Focus Device // Plasma Phys. Reports. – 2019. – Vol.45. – P.821-829.

18 Bhuyan H., et al. Magnetic probe measurements of current sheet dynamics in a coaxial plasma accelerator // Meas. Sci. Technol. – 2003. – Vol.14. – P.1769-1776.

19 Dosbolayev M., Raiymkhanov Zh., Tazhen A., Ramazanov T. Experimental Investigation of the Properties of Plasma-Dust Formations on Pulsed Plasma Accelerator // IEEE Transaction on plasma sci. – 2019. – Vol.47. – P.3047-3051.

20 Tazhen A.B., Dosbolayev M.K., Raiymkhanov Zh., Ramazanov T.S. Generation and Diagnostics of Pulse Plasma Flows // Plasma Phys. Reports. – 2020. – Vol.46. – P. 465-471.

21 Dosbolayev M.K., Raiymkhanov Zh., Tazhen A.B., Ramazanov T.S. Impulse Plasma Deposition of Carbon Nanoparticles // Acta Physica Polonica A. – 2019. – Vol.136. –P.348-350.

22 Tazhen A.B., Nurbolat K., Dosbolayev M.K. Spectroscopic diagnostic of a pulsed plasma flow // Journal of Peos. – 2018. – Vol.20. – P.45-51.

23 Utegenov A.U., Tazhen A.B., Rayimkhanov Zh.R., Kambarov A.A. Heat erosion of the graphite target under effects of intensive pulse plasma flow // Recent Contributions to Physics. – 2018. – Vol.4. P. – 34-40.

24 Tazhen A.B., Rayimkhanov Zh.R., Dosbolayev M.K., Ramazanov T.S. Obtaining and diagnostics of pulse plasma flows // Uspekhi prikladnoi fiziki. – 2019. – Vol.5. – P.463-471.

25 Dosbolayev M.K., Utegenov A.U., Tazhen A.B., Ramazanov T.S., Gabdullin M.T. Dynamic properties of pulse plasma flow and dust formation in the pulsed plasma accelerator // News Nat. Acad. Sci. Republic Kazakhstan. – 2016. – Vol.310. – P. 48-87.

References

1 H.R. Yousefi, W. Thornhill, J.I. Sakai, Y. Nishino, H. Ito, K. Masugata. Iranian Phys. Journal 2, 17-20 (2009).

2 E.J. Lerner, S.K. Murali, A.M. Blake, D.M. Shannon, F.J.V. Roesse. Nukleonika 57, 205-209 (2012).

3 M.K. Dosbolayev, A.U. Utegenov, A.B. Tazhen, and T.S. Laser and Particle Beams 35, 741-749 (2017). .

4 K. Zdunek, K. Nowakowska-Langier, R. Chodun, S. Okrasa, M. Rabinski, J. Dora, P. Domanowski, J. Halarowicz. Journal of Phys.: Conference Series 564, 012007 (2014).

5 V.A. Gribkov, I.V. Borovitskaya, E.V. Demina, E.E. Kazilin, S.V. Latyshev, S.A. Maslyaev, V.N. Pimenov, T. Laas, M. Paduch, S.V. Rogozhkin. Matter and Radiation at Extremes 5, 045403 (2020).

6 S.R. Chung, R.A. Behbahani, C. Xiao. Incorporating Plasma Sci. and Plasma Techn. 175, 1015-1020 (2020).

7 J. Jain, J. Moreno, S. Davis, B. Bora, C. Pavez, G. Avaria, L. Soto. Results in Phys. 16, 102915 (2020).

8 F. Castillo-Mejía, I. Gamboa-de Buen, J.J.E. Herrera-Velázquezand, J. Rangel-Gutiérrez. Journal of Phys.: Conference Series 511, 012021 (2014).

9 M. Scholz, B. Bienkowska, I. Ivanova-Stanik, L. Karpinski, R. Miklaszewski, M. Paduch, W. Stepniewski, K. Tomaszewski. Czechoslovak Journal of Phys. 54, C170-185 (2004).

10 P. Kubes, M. Paduch, J. Cikhardt, B. Cikhardtova, D. Klir, J. Kravarik, K. Rezac, E. Zielinska, M.J. Sadowski, A. Szymaszek, K. Tomaszewski, D. Zaloga. Phys. of Plasmas 24, 032706 (2017).

11 P. Kubes, M. Paduch, J. Cikhardt, D. Klir, J. Kravarik, K. Rezac, B. Cikhardtova, J. Kortanek and E. Zielinska. Plasma Phys. and Controlled Fusion 58, 045005 (2016).

12 J.X. Liu, J. Sears, M. McMahon, K. Tummel, C. Cooper, D. Higginson, B. Shaw, A. Povilus, A. Link, A. Schmidt. Plasma Phys. 1-8 (2016).

13 J. Narkis, E.N. Hahn, D.R. Lowe, D. Housley, F. Conti, F.N. Beg. Physics of Plasmas 28, 022707 (2021).

14 A. Beresnyak, J. Giuliani, S. Richardson, S. Jackson, S. Swanekamp, J. Schumer, R. Commisso, D. Mosher, B. Weber. IEEE Transactions on Plasma Science 46, 3881 – 3885 (2018).

15 S.H. Saw, M. Akel, P.C.K. Lee, S.T. Ong, S.N. Mohamad, F.D. Ismail, N.D. Nawi, K. Devi, R.M. Sabri, A.H. Baijan, J. Ali, S. Lee. Journal of Fusion Energy 31, 1-6 (2012).

16 D. Piriaei, S. Javadi, T.D. Mahabadi, H.R. Yousefi, A. Salar Elahi, and M. Ghoranneviss. Physics of Plasmas 24, 043504 (2017).

17 H.A. El-Sayeda, T.M. Allama, H.M. Soliman. Plasma Phys. Reports 45, 821-829 (2019).

18 H. Bhuyan et al. Meas. Sci. Technol. 14, 1769-1776 (2003).

19 M. Dosbolayev, Zh. Raiymkhanov, A. Tazhen, T. Ramazanov. IEEE Transaction on plasma sci. 47, 3047-3051 (2019).

20 A.B. Tazhen, M.K. Dosbolayev, Zh. Raiymkhanov, T.S. Ramazanov. Plasma Phys. Reports 46, 465-471 (2020).

21 M.K. Dosbolayev, Zh. Raiymkhanov, A.B. Tazhen, T.S. Ramazanov. Acta Physica Polonica A 136, 348-350 (2019).

22 A.B. Tazhen, K. Nurbolat, M.K. Dosbolayev. Journal of Peos 20, 45-51 (2018).

23 A.U. Utegenov, A.B. Tazhen, Zh.R. Rayimkhanov, A.A. Kambarov, Recent Contributions to Physics, 4, 34-40 (2018).

24 A.B. Tazhen, Zh.R. Rayimkhanov, M.K. Dosbolayev, Ramazanov T.S. Uspekhi prikladnoi fiziki 5, 463-471 (2019).

25 M.K. Dosbolayev, A.U. Utegenov, A.B. Tazhen, T.S. Ramazanov, M.T. Gabdullin News Nat. Acad. Sci. Republic Kazakhstan 310, 48-87 (2016).